

# Shape Effects in $E2$ Transition Rates from $Z \approx 76$ High-Spin Isomers

**P.M. Walker**

Department of Physics, University of Surrey, Guildford GU2 7XH, United Kingdom

Received 30 September 2017

**Abstract.** It is well known that high- $K$  isomers have strongly hindered electromagnetic decay rates. However, the situation is more subtle in shape-transition regions, where there are competing high-spin isomers associated with shape changes. Nevertheless, a previous analysis of  $E2$  decay rates from isomers in  $N \approx 76$  ( $A \approx 130$ ) nuclides enabled a degree of separation to be made between high- $K$  prolate states and low- $K$  oblate states. The analysis exploited the dependence of  $E2$  reduced hindrance factors,  $f_\nu$ , on the product of the valence nucleon numbers,  $N_p N_n$ . The present work investigates the application of these ideas to data for neutron-rich  $Z \approx 76$  ( $A \approx 180$ ) nuclides. Despite few such isomer data being available, it is found that the reduced hindrance factors can be used to help in distinguishing between three different  $E2$ -transition types. In particular, the decays from high- $K$  prolate isomers to the ground-state band are more hindered than the corresponding decays from low- $K$  oblate isomers. Other decays from low- $K$  oblate isomers have collective  $E2$  transition rates. These features may be helpful in future studies of nuclides in the neutron-rich  $Z \approx 76$  region.

PACS codes: 21.10.-k, 21.60.-n, 23.20.Lv, 27.70.+q, 27.80.+w

## 1 Introduction

Understanding the interplay between single-particle and collective degrees of freedom is an enduring theme of nuclear structure physics, exemplified by structural changes along the *yrast* line, i.e. the locus of states at minimum energy as a function of increasing angular momentum. For example, the rotational discontinuity known as *backbending* can usually be interpreted as being due to the alignment with the rotation of a pair of high- $j$  nucleons, driven by the Coriolis force [1]. In contrast, the  $A \approx 180$  deformed region has examples where deformation-aligned states, the high- $K$  isomers, become *yrast* [2]. Both of these alignment modes are almost always associated with prolate nuclear shapes. They were already identified in the 1970's, and considerable further work has clarified many aspects of the phenomena [3,4]. Meanwhile, a third kind of structural

change, predicted in the 1970's to occur at about  $26 \hbar$  in  $^{180}\text{Hf}$  [5], has hardly been explored. Named “giant backbending”, the rotational discontinuity is due, at least in theory, to a drastic change from prolate collective rotation to oblate collective rotation, driven by rotation alignment in the oblate well. Indeed, some suggestive experimental evidence has been found in the predicted nuclide [6]. Meanwhile, additional theoretical calculations [7] have pointed to the reinforcing effects of protons and neutrons, when their Fermi surfaces are both high (but not too high) in their respective shells, favouring the coexistence of oblate rotation-aligned states with prolate deformation-aligned states.

Related experimental work includes studying the neutron-rich hafnium isotopes, where the oblate mode is predicted to occur at lower energy [7, 8], but access is more difficult; and studying higher- $Z$  nuclides, where access is easier, but triaxiality becomes an important issue [4, 9]. However, the situation is complex, because there is coexistence of the three modes (prolate non-collective, prolate collective, and oblate collective [7]) and isomerism can be due to shape changes as well as  $K$  changes. Moreover, when experimental information is incomplete, there may be no *a priori* way to distinguish between them. Notably, while isomers are able to provide sensitive access to neutron-rich nuclides, especially when combined with in-flight separation techniques, this can come at the cost of no longer being able to observe the “prompt” rotational-band structures, so that key information may be missing. In order to explore these aspects, the present work builds on the existing knowledge of  $K$ -forbidden transition rates [4, 10–12]. An interpretation of  $E2$  reduced hindrance factors is suggested that could be helpful in distinguishing between the shape and  $K$  changes involved.

## 2 K-Forbidden Transitions

The  $K$  quantum number represents the projection of the total angular momentum on the symmetry axis of a deformed nucleus, usually with prolate shape. Since collective rotation generates angular momentum perpendicular to the symmetry axis, the  $K$  value in a rotational band is approximately constant, and its value is that of the bandhead angular momentum. Nevertheless,  $K$  mixing occurs due to the Coriolis force, which tends to align single-particle angular momenta along the collective rotation axis [1].

A key feature of a high- $K$  band is that its bandhead can be isomeric because of significant  $K$ -value changes in its electromagnetic decay. This is due to the vector property of angular momentum, requiring that the multipole order,  $\lambda$ , of the decay radiation, should not be smaller than the  $K$ -value change,  $\Delta K$ , thus specifying the  $K$ -selection rule,  $\Delta K \leq \lambda$ . In practice,  $K$  mixing leads to violations of the  $K$ -selection rule, and so-called “ $K$ -forbidden” transitions are hindered, rather than strictly forbidden. It is then convenient to define the degree of forbiddenness,  $\nu = \Delta K - \lambda$ , and the reduced hindrance,  $f_\nu = (F_W)^{1/\nu}$ ,

## Shape Effects in $E2$ Transition Rates from $Z \approx 76$ High-Spin Isomers

where  $F_W$  is the Weisskopf hindrance factor for a transition. In this way, there is allowance for the transition energy and multipole character, and it is the  $f_\nu$  value that contains the important physics [4, 12].

### 3 Dependence of $E2$ Reduced Hindrance on $N_p N_n$

In the present work, the focus is on  $E2$  transitions in even-even nuclides in the  $A \approx 170 - 190$  region. For two-quasiparticle isomers, the systematic and near-monotonic dependence of  $f_\nu(E2)$  on the product of the valence nucleon numbers,  $N_p N_n$ , is a useful starting point, which was introduced by Walker [10] and updated by Swan et al. [13]. (Note that Casten had already shown the importance of the  $N_p N_n$  parameterisation [14].) The possibility to extend the mass range to include weakly deformed nuclides in the  $A \approx 130$  region was discussed by Walker and Schiffer [11]. That work is particularly relevant here, because of its consideration of rotation-aligned oblate isomers which, if treated on the same footing as  $K$  isomers, give apparent  $f_\nu$  values somewhat lower than those expected for  $K$  isomers.

For isomers in the  $A \approx 170 - 190$  region with  $N_p N_n < 200$ , reduced hindrances are shown in Figure 1 (see ref. [13] for higher values of  $N_p N_n$ ). Numerical values are given in Table 1. The principal features of Figure 1 can be divided into three parts, according to the symbols used:

- (i) The high- $K$  isomers, represented by filled squares;
- (ii) The less-hindered transitions, represented by filled circles; and
- (iii) The collective transitions, represented by open circles.

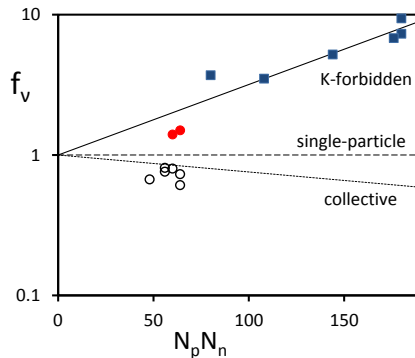


Figure 1. (color online) Reduced hindrance,  $f_\nu$ , as a function of the product of the valence nucleon numbers,  $N_p N_n$ , for  $E2$  transitions from two-quasiparticle states even-even nuclides in the  $A \approx 170 - 190$  region. The lines are to guide the eye, approximately representing  $K$ -forbidden, single-particle and collective transitions, as labelled. The data are from Kondev et al. [12] and are discussed in the text. Numerical values are given in Table 1. Statistical errors are smaller than the data points.

Table 1. Weisskopf hindrance factors,  $F_W$ , and reduced hindrances,  $f_\nu$ , for  $E2$  decays from two-quasiparticle states in the  $A \approx 170 - 190$  region, with  $N_p N_n < 200$ , as illustrated in Figure 1. The tabulation is in order of increasing  $N_p N_n$ . In the calculation of  $f_\nu$ , the initial state is assumed to have  $K_i = J_i$  and the final state to have  $K = 0$ . Thus, in each case, the degree of forbiddenness is taken to be  $\nu = K_i - 2$ . The  $\gamma$ -ray branching ratios,  $B_\gamma$ , are relative to the total decay intensity, which includes electron conversion. The data are from Kondev et al. [12].

Nuclide	$J_i^\pi$	$N_p N_n$	$E_\gamma$ (keV)	$T_{1/2}$	$B_\gamma$ (%)	$F_W$	$f_\nu$
$^{192}\text{Pt}$	$12^+$	48	105	2.6 ns	20	0.019	0.67
$^{190}\text{Pt}$	$12^+$	56	123	1.4 ns	3.8	0.12	0.81
$^{190}\text{Pt}$	$12^+$	56	191	1.4 ns	62	0.066	0.76
$^{192}\text{Os}$	$12^+$	60	112	1.4 ns	2.8	0.10	0.80
$^{192}\text{Os}$	$12^+$	60	446	1.4 ns	13	23	1.4
$^{188}\text{Pt}$	$12^+$	64	108	0.66 ns	16	0.0067	0.61
$^{188}\text{Pt}$	$12^+$	64	147	0.66 ns	11	0.044	0.73
$^{188}\text{Pt}$	$12^+$	64	373	0.66 ns	1.2	43	1.5
$^{190}\text{W}$	$8^+$	80	694	111 ns	82	$2.6 \times 10^3$	3.7
$^{184}\text{Os}$	$10^+$	108	1092	24 ns	19	$2.2 \times 10^4$	3.5
$^{182}\text{W}$	$10^+$	144	1087	1.3 $\mu\text{s}$	39	$5.4 \times 10^5$	5.2
$^{178}\text{W}$	$6^+$	176	1322	3.0 ns	58	$2.2 \times 10^3$	6.8
$^{172}\text{Hf}$	$6^+$	180	1376	4.8 ns	31	$7.8 \times 10^3$	9.4
$^{180}\text{Hf}$	$6^+$	180	1394	2.8 ns	56	$2.8 \times 10^3$	7.3

It is only for the high- $K$  isomers that the use of reduced-hindrance ( $f_\nu$ ) values is accepted practice. Nevertheless, the following discussion gives some justification for extending the numerical treatment to a wider range of states.

Considering first the high- $K$  isomers, each is the bandhead of a rotational  $\Delta I = 1$  sequence, characteristic of high- $K$ , deformation-aligned structure. The approximately monotonic dependence of  $f_\nu$  on  $N_p N_n$  has been presented previously [10, 13], and extends up to  $N_p N_n = 264$  for  $^{174}\text{Yb}$ , where the  $E2$  decay of a  $K^\pi = 6^+$  isomer has  $f_\nu = 350$  [12]. (However, future work may find exceptions, as seen for the corresponding  $M1$  reduced hindrances in  $^{172}\text{Er}$  [12] and  $^{170}\text{Dy}$  [15]). The surprisingly simple  $f_\nu$  dependence seems to come from a combination of Coriolis  $K$  mixing and departures from axial symmetry [10]. In Figure 1, the full line through the data points is largely to guide the eye, with the  $f_\nu = 1$  intercept consistent with the naïve expectation that  $K$  hindrance vanishes for closed-shell nuclei with spherical shape.

Secondly, there are data which show significant  $E2$  hindrance, but less than might be expected for  $K$ -forbidden transitions, at least according the simple dependence discussed in the previous paragraph. There are only two data points in this category, for specific  $E2$  decays in  $^{188}\text{Pt}$  and  $^{192}\text{Os}$ . In each case, the decay is from the  $J^\pi = 12^+$  bandhead of a  $\Delta I = 2$  sequence [16–18], giving the appearance of a rotation-aligned structure. The decay goes to the  $J^\pi = 10^+$

## Shape Effects in $E2$ Transition Rates from $Z \approx 76$ High-Spin Isomers

member of the ground-state band. For the purpose of comparison with the other decays (Figure 1) the  $J^\pi = 12^+$  bandhead is treated as a  $K = 12$  state, so that its  $\Delta K = 12$ ,  $E2$  decay has  $\nu = 10$ . The two  $f_\nu$  values are then close to unity (1.5 and 1.4, respectively). Nevertheless, their Weisskopf hindrance factors are arguably still significant (43 and 23, respectively) and certainly not collective. In each case, the  $E2$  hindrance could be caused by the configuration change (from rotation-aligned  $(i_{13/2})^2$  neutron structure [16, 18, 19] to the vacuum configuration) or by a shape change (from oblate to triaxial) or by a combination of both.

Finally, in four nuclides,  $^{192}\text{Os}$ ,  $^{188}\text{Pt}$ ,  $^{190}\text{Pt}$  and  $^{192}\text{Pt}$  [12], there are six decays where the  $E2$  hindrance is less than unity, with  $0.61 \leq f_\nu \leq 0.81$  in Figure 1 (i.e. treating them as  $\Delta K = 12$  transitions, for the purposes of comparison in the same figure). These transitions have collective character, with  $B(E2)$  values ranging from 8 to 150 Weisskopf units (W.u.). With one exception, the decay from the  $J^\pi = 12^+$ ,  $(i_{13/2})^2$  neutron structure goes to a  $J^\pi = 10^+$  state that is not a member of the ground-state band. The character of the  $J^\pi = 10^+$  state could be of  $(i_{13/2})^2$  neutron character with less than full alignment, or of fully-aligned  $(h_{11/2})^2$  proton character (see, for example, the discussion of Levon et al. [20]) or a mixture of the two. Both the aligned and partially-aligned structures would be associated with oblate shape, so that the  $E2$  transition does not involve a substantial shape change. This may be an important consideration for understanding the transition collectivity. The exception is the 123-keV transition in  $^{190}\text{Pt}$ , from the  $J^\pi = 12^+$  state to the  $J^\pi = 10^+$  member of the ground-state band. The collectivity in this case ( $1/F_W \approx 8$  W.u.) is likely to be due to an interaction of the populated state with another  $10^+$  state that is only 68 keV lower in energy, i.e. there is a chance near-degeneracy that leads to enhanced configuration mixing. The 191-keV transition to that other  $10^+$  state has greater collectivity ( $\approx 15$  W.u.).

The nuclides  $^{192}\text{Os}$  and  $^{188}\text{Pt}$  are notable in that, in the same nuclide, both collective and non-collective  $12^+ \rightarrow 10^+$ ,  $E2$  transitions are observed.

## 4 Discussion

In the previous section,  $E2$  transitions from two-quasiparticle isomers were treated in a common framework, which was based on accepted practice for high- $K$  isomers. Although this is an unconventional procedure for the analysis of rotation-aligned states, it nevertheless enables a range of isomeric  $E2$  transitions to be presented on the same graph. In this way, three types of isomeric transition can be distinguished, albeit with a limited number of data points. As already pointed out, the analysis builds on earlier work that looked at similar features in the  $A \approx 130$  region [11].

A key step is now to recognise that, even without the observation of a rotational

band associated with a given isomer, the  $E2$  reduced hindrance ( $f_\nu$ ) gives the possibility to determine the character of the initial state – either low- $K$  oblate (rotation aligned), or high- $K$  prolate (deformation aligned). This is significant because experimental information for neutron-rich nuclei is difficult to obtain, and in many cases depends on the in-flight separation of isomeric states, which subsequently decay by  $\gamma$ -ray emission (see, for example, Ref. [15]). In such circumstances, the prompt radiations typically remain unobserved. Therefore, in the search for oblate states in the neutron-rich hafnium isotopes (for example) an analysis of the type presented here may be useful.

The isomer half-lives can be crucial, because the flight times needed for nuclide identification are typically a few hundred nanoseconds. At first sight this is a particular problem for the oblate rotation-aligned isomers, which, in Table 1, have half-lives close to 1 ns. However, substantially longer half-lives can be anticipated in more-strongly deformed nuclides, such as the hafnium isotopes. Consider  $^{188}\text{Hf}$ , where  $N_p N_n = 100$ , and  $f_\nu \approx 2$  can be expected from Figure 1 for an oblate  $J^\pi = 12^+$  state. In that case, a 500-keV  $E2$  transition to the ground-state band would have a partial half-life of about 300 ns, which is long enough for in-flight separation techniques to be employed. Of course, other states might be populated in the decay, reducing the isomer half-life, but oblate isomers with several-hundred nanosecond half-lives do at least appear to be possible.

For comparison, a prolate  $K^\pi = 12^+$  state in  $^{188}\text{Hf}$  would be expected (from Figure 1 at  $N_p N_n = 100$ ) to decay to the  $10^+$  member of the ground-state band with  $f_\nu \approx 3$ , leading to a partial  $\gamma$ -ray half-life of about  $15 \mu\text{s}$  for a 500-keV  $E2$  transition, i.e. a factor of 50 longer than the corresponding oblate decay. It is hoped that such differences will be helpful in distinguishing between isomers with either prolate high- $K$  character or oblate low- $K$  character, and hence in enabling the structural properties the yrast line to be determined.

## 5 Conclusion

The decay hindrance factors for  $E2$  transitions from two-quasiparticle isomers in  $A = 170 - 190$  even-even nuclides have been investigated. When expressed in terms of  $f_\nu$  as a function of  $N_p N_n$ , it has been argued that three types of  $E2$  decay can be distinguished, two of which populate the ground-state band and are hindered. These two originate from either prolate deformation-aligned isomers, or oblate rotation-aligned isomers. The significant differences in reduced hindrance factors can help to identify these modes, and thus establish the nature of the yrast line.

## Acknowledgments

This research has been supported by the United Kingdom Science and Technology Facilities Council under grant No. ST/L005743/1, and the Bulgarian National Science Fund under contract No. DFNI-E02/6.

## References

- [1] F.S. Stephens (1975) *Rev. Mod. Phys.* **47** 43.
- [2] S. Åberg (1978) *Nucl. Phys.* **306** 89.
- [3] M.A. Riley, J. Simpson, E.S. Paul (2016) *Phys. Scr.* **91** 123002.
- [4] G.D. Dracoulis, P.M. Walker, F.G. Kondev (2016) *Rep. Prog. Phys.* **79** 076301.
- [5] R.R. Hilton, H.J. Mang (1979) *Phys. Rev. Lett.* **43** 1979.
- [6] U.S. Tandel et al. (2008) *Phys. Rev. Lett.* **101** 182503.
- [7] F.R. Xu, P.M. Walker, R. Wyss (2000) *Phys. Rev. C* **62** 014301.
- [8] M.W. Reed et al. (2010) *Phys. Rev. Lett.* **105** 172501.
- [9] L.M. Robledo, R. Rodriguez-Guzman, P. Sarriguren (2009) *J. Phys. G* **36** 115104.
- [10] P.M. Walker (1990) *J. Phys. G* **16** L233.
- [11] P.M. Walker, K. Schiffer (1991) *Z. Phys. A* **338** 239.
- [12] F.G. Kondev, G.D. Dracoulis, T. Kibédi T (2015) *At. Data Nucl. Data Tables* **103-104** 50.
- [13] T.P.D. Swan, P.M. Walker, Zs. Podolyák, M.W. Reed, G.D. Dracoulis, G.J. Lane, T. Kibédi, M.L. Smith (2011) *Phys. Rev. C* **83** 034322.
- [14] R.F. Casten (1985) *Phys. Lett. B* **152** 145.
- [15] P.-A. Söderström et al. (2016) *Phys. Lett. B* **762** 404.
- [16] L. Richter, H. Backe, F. Weik, R. Willwater (1979) *Nucl. Phys. A* **319** 221.
- [17] S. Mukhopadhyay et al. (2014) *Phys. Lett. B* **739** 462.
- [18] G.D. Dracoulis et al. (2013) *Phys. Lett. B* **720** 330.
- [19] P.M. Walker, F.R. Xu (2006) *Phys. Lett. B* **635** 286.
- [20] A.I. Levon, Yu.V. Nosenko, V.A. Onischuk, A.A. Schevchuk, A.E. Stuchbery (2006) *Nucl. Phys. A* **764** 24.